A mechanism for damage formation in GaN during rare earth ion implantation at medium range energy and room temperature

P. Ruterana, B. Lacroix, K. Lorenz

A mechanism for damage formation in GaN during rare earth ion implantation at medium range energy and room temperature

P. Ruterana and B. Lacroix

CIMAP, UMR 6252 CNRS ENSICAEN, CEA, UCBN, 6 Boulevard du Maréchal Juin, 14050 CAEN, France

K. Lorenz

Instituto Tecnológico e Nuclear, EN 10, 2686-953 Savacém, Portugal

Abstract

A detailed investigation of the crystallographic damage has been carried out in GaN following 300 keV ion implantation at room temperature by varying the fluence of Eu from a few $*10^{13}$ to $5*10^{16}$at/cm^2. It is shown that when a threshold fluence around $2x10^{15}$at/cm^2 is reached, nanocrystallization takes place from the surface, subsequent to the formation of a planar defects network composed of basal and prismatic stacking faults. This network starts to form at the lowest analyzed fluence mostly around the mean projected range and when the fluence increases, it propagates towards the surface, reaching it just before the nanocrystallization initiation. A model based on the mechanical breakdown of the GaN wurtzite structure mediated by the prismatic stacking faults is proposed.

1. Introduction

The usual picture of damage formation in materials by ion implantation in the medium energy range (10 keV - 1 MeV) is through atomic displacements in the host material by ballistic collision cascades which ends up by breaking down the crystalline structure towards amorphization. For more than 10 years now, rare earths (REs) doping of GaN has received a great interest due to expected promising applications in optoelectronics and photonics[1]. Until now, RE implantation has been mainly used to investigate the fundamental properties of the RE-GaN system[2-3]. A continuous research effort is carried out in order to determine the most effective conditions for implantation and annealing of GaN[4-6]. Concerning the damage formation and accumulation in GaN, early reports on Ca and Ar implantation at liquid nitrogen temperature indicated that the formation of an amorphous layer in GaN by high fluence implantation started at the mean projected range (100 nm at 180 keV) and then extended towards the surface[7]. Most recent investigations for low and room temperatures implantations have shown that the 'amorphization' of GaN is a layer by layer process starting from the surface[8, 9]. However, in contrast to Si or GaAs, GaN is considered as difficult to amorphize by ion bombardment. This has been attributed to an efficient dynamic annealing which takes place during implantation[8,10]. The planar defects have been observed independently of the ion, fluence, energy and implantation temperature. They appear to represent the structural defect that are the most characteristic for GaN bombarded with ions under a wide range of implantation conditions[9].

GaN doping with rare earth ions started quite early[11] with Er, but only 1.5 µm emission was obtained after 600-700°C annealing. Later on, up to 10 times increase in luminescence was reported to take place in Eu implanted GaN after annealing between 1100°C to 1300°C[12]. Subsequently transmission electron microscopy (TEM) results showed that this high luminescence might be correlated with the decrease in the planar defects density inside the implanted area by annealing at temperatures above 1100°C[13].

Earlier, it was suggested that the planar defects that form during the ion implantation of GaN may constitute 'nucleation sites' for 'amorphization' when the implanted ion fluence is increased above some critical value during bombardment [9]. In our previous work, we have shown that these planar defects were made of basal and prismatic stacking faults[14].

In this study it was found that the highly damaged surface region was not amorphous but consisted of randomly oriented nano-crystallites. Then, by following the evolution of the stacking faults versus the ion fluence, we are able to point out the critical role of the prismatic stacking faults in the generation of the nanocrystalline layer starting at the implanted GaN surface. In the following, a model is proposed for the formation of this layer which seems to mechanically relieve the strain which is generated during ion implantation.

2 Experimental

Er, Eu or Tm rare earth ions were implanted in 2 μm thick GaN layers grown on (0001) sapphire by metal organic chemical vapour deposition. The implantation was carried out at room temperature (RT) with an energy of 300keV and fluences of $7x10^{13}$ to $5x10^{16}$ at/cm^2. The corresponding simulated profile of implanted ions using the SRIM program gives a mean projected range (Rp) of 55 nm, with a full width at half maximum of 46 nm. Conventional (TEM) and high resolution transmission electron microscopy (HRTEM) was carried out on cross-sections thinned down to 100 μm by mechanical grinding and dimpled down to 15 μm, as well as by tripod polishing until electron transparency. In some cases, the electron transparency was achieved by ion milling at 5 kV at room temperature as well as by keeping the sample holder at the liquid nitrogen temperature using the GATAN precision ion polisher (PIPS) at an incidence angle of 5 degrees. Thus doing, we have been able to notice that the ion milling process did not have any particular effect in the layer structure. CTEM was performed with a JEOL 2010 microscope operating at 200 keV and the HRTEM was carried out in a JEOL 2010FEG instrument operating at 200 keV with a point resolution of 0.2 nm.

3. Results

As now appears to become established, the formation of defects due to ion implantation in GaN does not necessarily follow a simple accumulation of vacancies and interstitials within the damaged area, followed by the formation of an amorphous layer due to the collapse of the crystalline structure starting either from the maximum of nuclear energy deposition or from the maximum of the implanted ion profile (Rp: projected range), as first pointed out in 140 keV Zn implantation[15]. At higher energies and/or ion atomic number, the generated damage structure is more complex; indeed, surface and buried damaged layers have been reported[16]. As shown in the following, the dominant extended defects that appear first are mainly basal stacking faults (BSFs) of I_1= 1/6 $[20\bar{2}3]$ type, which propagate to the layer surface through an easy formation of prismatic $\{11\bar{2}0\}$ stacking faults. The interacting combination of the two stacking fault systems is shown to give rise to non damaged nano crystalline areas which eventually form a highly disordered surface layer.

3.1 Point defects accumulation

By imaging in 0002 weak beam conditions it is possible to reveal the atomic displacements along the [0001] direction. Such contrast is related to clusters of interstitials or vacancies. The implantation generates visible damage by TEM even at the smallest investigated fluence of $7x10^{13}$ at/cm^2, as can be noticed in figure 1a; the displacements along the c axis are noticeable down to 80 nm depth. When the fluence is increased to $2x10^{15}$ at/cm^2, the damage contrast is visible down to 220 nm (fig. 1b), which is nearly three times deeper than after the lowest implantation fluence. Obviously, as the implantation fluence is increased, the damage density becomes high enough to give rise to visible contrast in TEM images deeper in the implanted layer.

3.2 A typical damage character

As can be noticed in g= $01\bar{1}0$ weak beam observations, a characteristic damage along the basal planes is formed which also increases with the fluence (Fig. 2): it is made of non continuous bright lines parallel to the layer surface. Almost not visible at the lowest analyzed fluence[17], the corresponding contrast runs as deep as about 200 nm at 10^{15} at/cm^2 (fig. 2, see vertical arrows). However, a closer examination of the figure towards the surface points out that the near surface region is almost defect free (white horizontal arrows). This is confirmed by the corresponding HRTEM observations which show that, after the implantation fluence of $1x10^{15}$ at/cm^2, the defects inside the basal lattice planes appear starting from a depth of 30 nm. As can be noticed in figure 3, the surface part of the sample is planar defect free: some of them have been underlined in the basal planes, and some connections inside the prismatic planes have also been marked with stars. The most observed planar defects are BSFs of I_1= 1/6 [$20\bar{2}3$] type; their length in the basal plane may be quite small, about 7 nm, and they easily fold out off the basal planes, giving rise to prismatic stacking faults (PSFs). Indeed, during the implantation of rare earth ions, the three types of basal stacking faults of the wurtzite structure are generated, but the I_1 SFs are predominant[14]. Of course, the defect system is complex: as shown in figure 4a, an I_1 stacking fault, from the left end of the micrograph, transforms to E=1/2[0001] by loosing its 1/3<$10\bar{1}0$> component (upward arrow). Subsequently, it takes back the basal component (downward arrow) to another I_1, which folds to a lower basal plane through a small PSF (white hexagon). The initial and final I_1 faults have the same displacement vector in the basal plane, whereas that of the intermediate I_1 is opposite. The PSFs which allow the I_1 faults to fold from one basal plane to another can be more or less extended vertically: 1c in figure 4a and more than 2c in figure 4b.

The contrast of the observed PSFs corresponds to the Drum atomic configuration ($D=1/2[10\bar{1}1]$)[18, 19] (see hexagons in figures 4a and b) and not the Amelinckx configuration[20].

From the lowest fluences ($7x10^{13}$ at/cm^2) to $2x10^{15}$ at/cm^2, the density of these defects is increased by 5 times[18], it then saturates above $2x10^{15}$ at/cm^2. An important point that needs to be noticed is that at $2x10^{15}$ at/cm^2, as can be seen in figure 5, the sample surface has now become rough, the peak to peak roughness can be as large as 10 nm (see black arrow), and, in contrast to the $1x10^{15}$ at/cm^2 fluence, the stacking fault system is now reaching the layer surface (see white arrow). It should also be noticed that very low concentrations of $I_2=1/3[10\bar{1}0]$ BSFs are generated[14]; this may be connected to their intrinsic nature, which is a pure displacement in the basal plane as opposed to the highest concentration of I_1 faults which have a component along the c axis. As can be seen in Table 1, the I_1 BSF and the Drum PSF exhibit the lowest formation energies in GaN[21,22]. Due to its component along c, the I_1 appears to easily fold into the prismatic plane, thus baring the Drum configuration; this is probably at the origin of the propagation of the whole stacking fault system towards the surface and may be the basis of the damage formation during the implantation of GaN.

3.3 Around the breakdown threshold of the crystalline structure

As it has been stated many times, for heavier ions, the chemical effects of implanted species should be negligible and an increase in the density of collision cascades strongly contribute to increase the level of implantation-produced lattice disorder in the bulk as well as the rate of layer by layer amorphization proceeding from the surface[8-10]. In order to check this mechanism for GaN, we have carried out implantations by attempting small steps in fluences at 2.5, 3, 3.5, 4, 4.7, $5.6x10^{15}$ at/cm^2 for the Eu ions. When the fluence has been increased from 2 to 2.5 $x10^{15}$ at/cm^2, a highly disturbed layer of ~25 nm has formed at the surface. As exhibited in figure 6, this layer is not amorphous: towards the bulk, the (0001) lattice fringes keep their perfect orientation

along the normal to the surface, with a more or less extended length. While, when moving to the surface, such atomic planes appear to have undergone misorientations. On this micrograph, which is a projection along $[11\bar{2}0]$ of the observed area, a number of moiré fringes are visible throughout the whole image (some have been marked with 'm'), and this is an evidence of the relative tilts between adjacent crystalline areas. Using the next two fluences, the structure of the generated surface does not change remarkably, taking into account the surface roughness, its thickness is seen to fluctuate between 22 and 26 nm and moiré fringes are still observed with extensions that may exceed 10 nm in length and with a tendency to decrease with the increase in fluence. A clear morphological change of the surface layer is seen to take place starting at $4x10^{15}$ at/cm^2, the layer is nanocrystalline all over (figure 7a) and moiré fringes are no more visible, the nanocrystallites are now small in size (~3-5 nm). The absence of moiré fringes is a strong indication that we now have large misorientations between adjacent small nanocrystalline areas. The average thickness of this surface layer now exceeds 30 nm, and its interface with the less damaged part of the bulk is more delineated (see white horizontal arrow). The surface roughness has also become reasonably small in comparison to the 2 to $3.5x10^{15}$ at/cm^2 fluence range (figs 5-6). A close examination point out that on both sides of this interface(figure 7b), numerous cubic stackings have formed (see black stars). From the interface towards the surface, the lattice planes mostly {0001} present a larger and larger misorientation (white arrows). Some well defined and independent nanocrystallites can be clearly pointed out especially close to the surface (see 1, 2 and 3 white marks). In between well defined nanocrystallites, very small areas may also exhibit quite random contrast (1 black arrows). This may indicate a possible presence of highly misoriented out of zone axis areas of sub-nanometer size that cannot be imaged with enough resolution by the used HRTEM equipment (~0.2 nm). These areas may be voids, or very small amorphous patches (<1 nm). Indeed, as can be noticed, there are lattice fringes throughout the whole layer. Of course, each lattice fringes series extends only on a few nanometers, indicating

that this area is composed of nanocrystallites which are misoriented from one another. Consequently, from such micrograph, it would be difficult to extract evidence of a mixture of broken crystals and an amorphous phase as has been proposed earlier by Ding et al.[15]. At the fluences of 4 to 4.7x10^{15} at/cm^2, the thickness of the nanocrystalline layer is almost multiplied by 3 from 32 nm to 90 nm; figure 8 shows the extension of the damage in GaN in the investigated conditions.

In the thickest nanocrystalline layers, it was possible to record selected area diffraction patterns, as shown in figure 9, where a simulated GaN powder pattern has been superimposed. We have only a spotty diagram of GaN with well defined rings of the wurtzite structure. The average nanocrystal diameter used for the simulation of the inserted powder pattern is of about 3-5 nm in complete agreement with the observation of HRTEM. Implantation at higher fluences in this channelled geometry does not lead to a formation of thicker damaged surface layers as can noticed in figure 8. This saturation is probably due to the used ion energy (300 keV) as well as the possible strong dechannelling which may occur as soon as the nanocrystallization is taking place.

From this observation, the degradation of the GaN structure during ion implantation of REs appears to take place in 4 steps:

I. From the lowest investigated fluences to 10^{15} at/cm^2, *the characteristic extended defects are BSFs and PSFs whose density increases monotonically with the fluence; this network stays buried below some 30 nm* (figure 3).

By 2x10^{15} at/cm^2, the density of the stacking fault system saturates and now reaches the surface, especially the I_1 BSFs and the PSFs with the Drum atomic configuration. Simultaneously, a typical roughness is formed at the implanted layer surface, with a peak to peak extension between 5 and 10 nm (see figure 6).

II. By $2.5x10^{15}$ at/cm^2, the crystalline structure is seen to break down within a depth of some 25 nm. *The resulting layer is rough, the peak to peak roughness is close to 10 nm, and it consists of misoriented nanocrystals having size higher than 10 nm as shown by the occurrence of moiré fringes (see 'm' in figure 6).*

When the fluence is increasing up to $4x10^{15}$ at/cm^2, a thickness of 32 nm is attained for the nanocrystalline layer, its roughness is strongly reduces (2-4 nm) and the nanocrystallites average size settles to less than 5 nm (figure 7a).

III. *Between 4 and $4.7x10^{15}$ at/cm^2, the thickness of the generated surface nanocrystalline layer is increased by a factor of 3 (figure 8).*

IV *Above $5x10^{15}$ at/cm^2, this thickness reached a maximum of about 90 nm, and even appears to slightly decrease (figure 8).*

This saturation is easily explained by the implantation energy limiting the ion range together with a decreased channelling of ions, and the apparent decrease of the nanocrystalline layer extension at higher fluences may probably be explained by a possible ion-induced surface sputtering[25]. Another characteristic feature that should be pointed out is the appearance of voids whose structure seems to be settled at the fluence $4.7x10^{15}$ at/cm^2. As pointed out in figure 7b, some small areas have been noticed to exhibit random contrast, and were qualified as possible 'nanovoids'. Now moving to an even thinner area of the same sample, it can be noticed in figure 10, that, obviously, we have misoriented nanocrystallites inside the highly damaged layer. Moreover, numerous voids are displayed; they are distributed all over this disordered layer, exhibit various geometries and their sizes vary from 1-2 nm to 5 nm (see black arrow). So, these observations are showing that in GaN, the highly damaged surface area resulting from rare earth ion implantation is not amorphous, but it is made of nanocrystallites which may be separated by nanometer size voids.

4. Discussion

In this work, a detailed investigation of the damage that form during Eu implantation in GaN at medium range energy (300 keV) and room temperature has been carried out, especially at the vicinity of the critical fluence for which the crystalline structure breaks down which has been shown to take place starting from the surface in comparable implantation conditions[9]. The motivation behind this study is the fact that in contrast to other semiconductors such as Si or SiC, the latest reports have pointed out the formation of nanocrystals within the surface damaged layer. In the first report of 2003, Ding et al. concluded that GaN[15], subsequent to Zn ion implantation of $3x10^{16}$ at/cm^2 at 140 keV, exhibited a thin surface layer composed of a mixture of amorphous material and broken crystals. Subsequently in a study of damage formation in GaN during the implantation of 2 MeV Au ions, Jiang et al. proposed a mechanism which consisted of structural transformation at higher fluences from a high concentration of dislocation loops to small crystalline domains with random orientations caused by lattice strains; followed by a complete amorphization due to an inefficient simultaneous recovery of point defects in the randomly oriented crystalline domains[23]. In the most recent report of the same group[24], Au ion implantation carried out at 60° incidence, at 2 MeV and low temperature (150 K) two typical morphologies were pointed out: 1. The so called “amorphous area” which exhibited atomic arrangement with sizes less than ~4 nm; it was suggested that the random orientation of such nanocrystals could be a proof that they might be formed as a consequence of ion assisted recrystallization of an amorphous phase. 2. High contrast nanocrystals were identified as cubic GaN phase. In the meantime, it was reported that during sputter deposition, GaN always deposits in the form of randomly stacked ~3nm size nanocrystals, and the amorphous GaN phase could only be attained when more than 15% of oxygen was codeposited[26]. As can be seen in Fig. 11, Eu implantation into silicon to a fluence of $7x10^{13}$ at/cm^2 is enough to give rise to amorphization where the completely random contrast points to a 100% disordering of the lattice in contrast to

our case as exhibited in figure 10. In this micrograph, a close examination shows a few correlated lattice fringes (see arrows) but always with an extension of close to 1 nm or less. So there remain at least two questions in order to explain the origin of this peculiar mode of damage in GaN during/subsequent to ion implantation:

1. GaN is considered by some authors as a material having an efficient dynamical annealing. What exactly is meant by the dynamical annealing in this instance (annihilation of interstitials and vacancies and formation of extended defects, formation of the nanocrystals, ...)?

2. What is the reason behind the nanocrystallization that starts at the GaN surface (surface trap of interstitials, strain relaxation…)?

In our latest report on the damage formation in GaN[6], it was shown by RBS/channelling, that the surface damage peak reached a relative defect density above 0.8 at $2x10^{15}$ at/cm^2. This is exactly when the stacking fault system reaches the GaN layer surface. This occurs following the saturation of the bulk damage peak above $1.2x10^{15}$ at/cm^2, and then a fast increase of the surface damage peak which saturates at a relative defect level of 0.9. The defect level for the studied fluence range was never seem to reach unity which would correspond to the amorphous level. An apparently important point which has not been taken into account in earlier studies is the parallel occurrence of the prismatic and basal stacking faults. As it was shown earlier, the Drum atomic configuration prismatic stacking fault may undergo volume expansion when subjected to strain for instance in the presence of dislocations[27]. From the diffraction pattern of the nanocrystalline area (fig.9), only the GaN wurtzite phase appears to be present. Moreover, as evidenced above, the observations around the nanocrystallization threshold show that the surface nanocrystallization starts by a breakdown within an initial depth of about 25 nm with more or less tilted crystallites of sizes up to 10 nm, as shown by the presence of moiré fringes. This settles then to nanocrystallites with sizes around 5 nm and misorientations which appear to be

decreasing from the surface towards the less damaged bulk area at about $4x10^{15}$ at/cm^2. At the next fluence of $4.7x10^{15}$ at/cm^2, the nanocrystallites size does not change any more, and the highly damaged layer thickness saturates due to the ion energy in combination probably with the dechannelling brought about by the simultaneous occurrence of the misoriented nanocrystals. So, one point that may be pointed out from the above observations is that at least for our implantation conditions, there does not seem to be any layer by layer amorphization which takes place from the surface. *Instead, we have a collapse of the crystalline structure into a nanocrystalline state, starting from a rough surface and a surface layer saturated with basal and stacking faults.* Therefore, one way of taking into account the above observations may be schematically seen in figure 12. We may assume that the often reported efficient dynamical[10] annealing of GaN corresponds to the formation of the observed network of BSFs and PSFs which starts at the around Rp, and increases in density with the fluence as shown schematically in figure 12a. In our implantation conditions, this network propagates then towards the surface versus the fluence, and reaches it at around $2x10^{15}$ at/cm^2. The above results show clearly that such propagation is due to the simultaneous formation of the two types of stacking faults: I_1 BSFs and PSFs. As can be seen in the figures, the areas limited by such a network are of nanometer size and do not exhibit any defects. *Therefore, such areas are most probably the seeds of the nanocrystals that result when the material breakdown* (figure 12b). With this model, it clear that the damage formation may not take place in two steps and *the earlier proposal of ion assisted recrystallization*[24], which has been suggested to explain the systematic occurrence of the nanocrystals, may not be necessary. This is also in agreement with the reported high stability of nanocrystalline GaN versus the amorphous phase[26].

5. Summary

During RT implantation at 300 keV, around a threshold fluence of around 2 x10^{15} Eu/cm^2, the high density stacking fault system made of mostly I_1 basal and prismatic stacking fault has propagated from Rp to the layer surface which has acquired a roughness of about 10 nm. When the fluence is further increased, the crystallographic system breaks down first slowly to a depth of about 25 nm into extended and misoriented nanocrystals, no layer by layer amorphization from the surface does seem to take place in GaN. The highly damaged surface layer is first made of extended nanocrystals (~10 nm) which settle to some 3-5 nm when the fluence is further increased. The proposed mechanism for this behaviour is a mechanical breakdown of the crystalline structure due to large strains from the implanted heavy ions. The breakdown is expected to come about through the relief of these strains by the volume expansion inside the prismatic stacking faults and this is at the origin of the nanocrystallization which takes place from the surface of GaN during the implantation of heavy ions.

Acknowledgement,

The authors acknowledge Dr. Florence Gloux for her contribution to this work

References

[1]D. S. Lee and A. J. Steckl, Appl. Phys. Lett. **80**, 1888(2002)

[2] S.J. Pearton, F. Ren, A.P. Zhang and K.P. Lee, Mater. Sci. Eng. R **30**, 55 (2000)

[3] M. Mamor, V. Matias, A. Vantomme, A. Colder, P. Marie and P. Ruterana, Appl. Phy. Lett. **85**, 2244 (2004)

[4]F. Gloux, P. Ruterana, K. Lorenz and E. Alves, Phys. Stat. Sol. (a) **205**, 68(2008)

[5] F. Gloux, P. Ruterana, K. Lorenz and E. Alves, Materials Science and Engineering B **146,** 204(2008)

[6] K. Lorenz, N.P. Barradas, E. Alves, S. Roqan, E. Nogales, R.W. Martin, K. P. O'Donnell, F. Gloux and P. Ruterana, J. Phys. D Appl. Phys. **42,** 165103 (2009)

[7] C. Liu, B. Mensching, M. Zitler, K. Volz, and B. Rauschenbach, Phys. Rev. B **57**, 2530 (1998)

[8] S. O. Kucheyev, J. S. Williams, C. Jagadish, J. Zou, and G. Li, Phys. Rev. B **62**, 7510 (2000)

[9] S.O. Kucheyev, J.S. Williams, C. Jagadish, J. Zou, G. Li and A.I. Titov, Phys. Rev. B **64**, 035202 (2001)

[10] S.O. Kucheyev, J.S. Williams and S.J. Pearton, Mater. Sci. Eng. R **33**, 51 (2001)

[11] R.G. Wilson, R.N. Schwartz, C.R. Abernathy, S.J. Pearton, N. Newman, M. Rubin, T. Fu and J.M. Zavada, Appl. Phys. Lett. **65**, 992 (1994)

[12] K. Lorenz, U. Wahl, E. Alves, S. Dalmasso, R. W. Martin, K. P. O'Donnell, S. Ruffenach and O. Briot, Appl. Phys. Lett. **85**, 2712 (2004)

[13]T. Wojtowicz, F. Gloux, P. Ruterana, K. Lorenz, E. Alves, Opti. Mat. **28**, 738 (2006)

[14]F. Gloux, T. Wojtowicz, P. Ruterana, K. Lorenz, E. Alves, J. Appl. Phys. **100**, 073520 (2006)

[15] F-R. Ding, W-H. He, A. Vantomme, Q. Zhao, B. Pipeleers, K. Jacobs, nd I. Moerman , Mat. Sci. in Semi. Processing **5**, 511(2003)

[16]M. Ishimaru_ Y. Zhang and W. J. Weber, J. Appl. Phys. 106, 053513 (2009)

[17] T. Wojtowicz, P. Ruterana, D.S. Lee, and A. Steckl, phys. stat. sol. (c) 2, No. 7, 2484 (2005)

[18]C. M. Drum, Philos. Mag. **11**, 313 (1964)

[19] P. Vermaut, P. Ruterana, and G. Nouet, Appl. Phys. Lett. **74**, 694(1999)

[20]H. Blank, P. Delavignette, R. Gevers, and S. Amelinckx, Phys. Status Solidi **7**, 747(1964)

[21] C. Stampfl and C.G. Van de Walle, Phys. Rev. B **57** (1998) R15052

[22] P. Ruterana, B. Barbaray, A. Bere, P. Vermaut, A. Hairie, E. Paumier, G. Nouet, A. Salvador, A. Botchkarev, and H. Morkoc, Phys. Rev. B **59**, 15917 (1999)

[23]W. Jiang , W.J. Weber , L.M. Wang , K. Sun , Nucl. Instr. and Meth. in Phys. Res. B 218 427(2004)

[24] I. T. Bae, W. Jiang, C. Wang, W. J. Weber and Y Zhang, J. Appl. Phys. **105**, 083514(2009)

[25] K. Lorenz, U. Wahl, E. Alves, E. Nogales, S. Dalmasso, R. W. Martin, K. P. O'Donnell, M. Wojdak, A. Braud, T. Monteiro, T. Wojtowicz, P. Ruterana, S. Ruffenach, O. Briot, , Optical Materials 28750 (2006).

[26]F. Budde, B. J. Ruck, A. Koo, S. Granville, H. J. Trodahl, A. Bittar, G. V. M. Williams, M. J. Ariza, B. Bonnet, D. J. Jones, J. B. Metson, S. Rubanov and P. Munroe, J. Appl. Phys. **98**, 063514 (2005)

[27] S Kret, P Ruterana and G Nouet, J. Phys.: Condens. Matter **12** 10249(2000)

Figure Captions

Figure 1: Weak beam micrographs (g=0002) of GaN layers implanted at 300keV and RT, with a fluence of a) 7×10^{13} Eu/cm^2 , b) of 2×10^{15} Eu/cm^2

Figure 2: a (01-10) weak beam micrograph of the GaN layer implanted with 10^{15} Eu at/cm^2, the horizontal arrows show the limit of the surface which does not exhibit basal stacking faults, the vertical arrows show the whole implanted layer as underlined by the presence of the stacking faults.

Figure 3: HRTEM image of GaN layers implanted at 300keV and RT, with the fluence of $1x10^{15}$ Eu/cm^2; the stacking fault system is buried within a depth of some 30 nm, the top defects are underlined (I1 in white, E in black, and some loops are also visible (E: black stars, I1: white stars). The surface roughness is quite reasonable (0.5-1.5 nm).

Figure 4: Formation of the various types of basal SFs and their folding into the prismatic plane through the Drum prismatic SF atomic configuration, a) From left side of the micrograph the I1 SF transforms into an E type SF, then back to another I1, this later fold into a lower c plane through the formation of a Drum configuration prismatic stacking fault (see hexagonal projection). b) the I1 basal stacking fault is shifted to another c plane at almost 1 nm distance through a longer prismatic stacking faults.

Figure 5: A HRTEM micrograph of the surface part of the GaN layer after ion implantation of Eu at $2x10^{15}$ at/cm^2, the stacking faults network is now reaching the surface (white arrow). The roughness of the layer is now of more than 10 nm.

Figure 6: The highly damaged surface layer after Eu implantation at 300 KeV, $2.5x10^{15}$ at/cm^2; the layer surface is still rough, the damaged layer exhibits many moiré fringes, some have been marked with (m).

Figure 7: At $2.5x10^{15}$ at/cm^2, a) the interface of the surface damaged layer is now more delineated (white arrow) and the surface roughness has decreased. b)Inside the nanocrystalline layer, the size of the nano grains varies from 3 to about 5 nm, the misorientations are seen to increase from the interface towards the surface where some c lattice fringes can even be vertical (white arrows). Some individual nanocrystals have been pointed out (numbers 1-3 in white), numerous cubic sequences are also noticeable (black stars), characteristic of the basal stacking faults. Small (~1nm) areas show an amorphous contrast, they may correspond to highly misoriented zones, voids, or amorphous patches (black arrow with number 1).

Figure 8: Thickness of the damaged layer versus the ion fluence, at 300 keV and RT

Figure 9: A diffraction pattern of the surface nanocrystalline layer formed by Eu $4.7x10^{15}$ cm^{-2} ions channelled implantation in GaN, in the insert, a simulated powder pattern with GaN crystallites diameter of 3-5 nm is displayed.

Figure 10: A HRTEM micrograph of the GaN layer following Eu implantation at RT, 300KeV with $4.7x10^{15}$ at/cm^2. Nanocrystallites are visible, no extended amorphous areas can be seen and voids have formed with sizes from 1 to 4-5 nm.

Figure 11. A HRTEM micrograph of a Si wafer following Eu implantation at RT, 300KeV with 7 $x10^{13}$ at/cm^2

Figure 12: The proposed model for the formation of the crystallographic damage in GaN, a) The stacking faults system, b) the break down of the crystalline structure through the strain relief by the volume expansion inside the prismatic stacking faults.

Table 1 : The theoretical formation energies of the stacking faults in GaN

Formation energy (meV/Å^2)	GaN
FEB I_1 [ref. 21]	10
FEB I_2 [ref. 21]	24
FEB E [ref. 21]	38
FEP DM [ref. 22]	22
FEP AM [ref. 22]	78

Figure 1

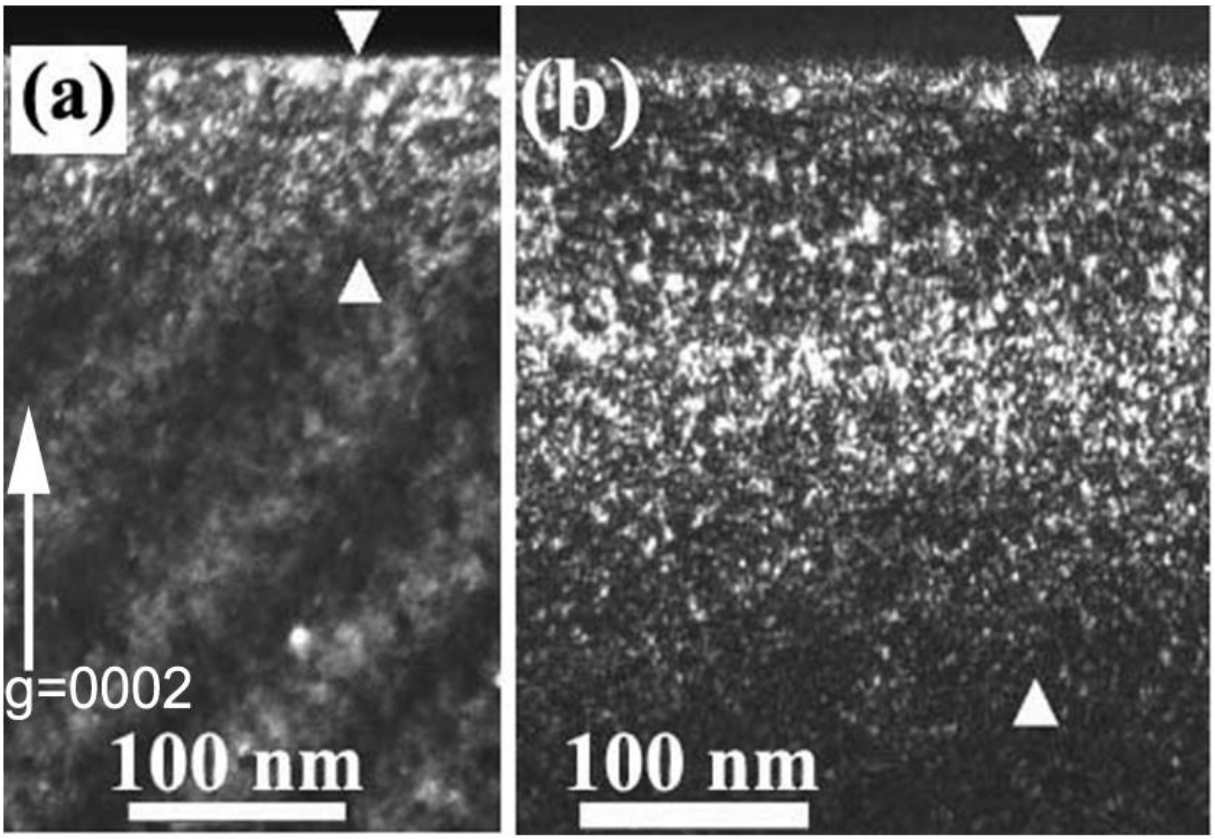

Figure 2

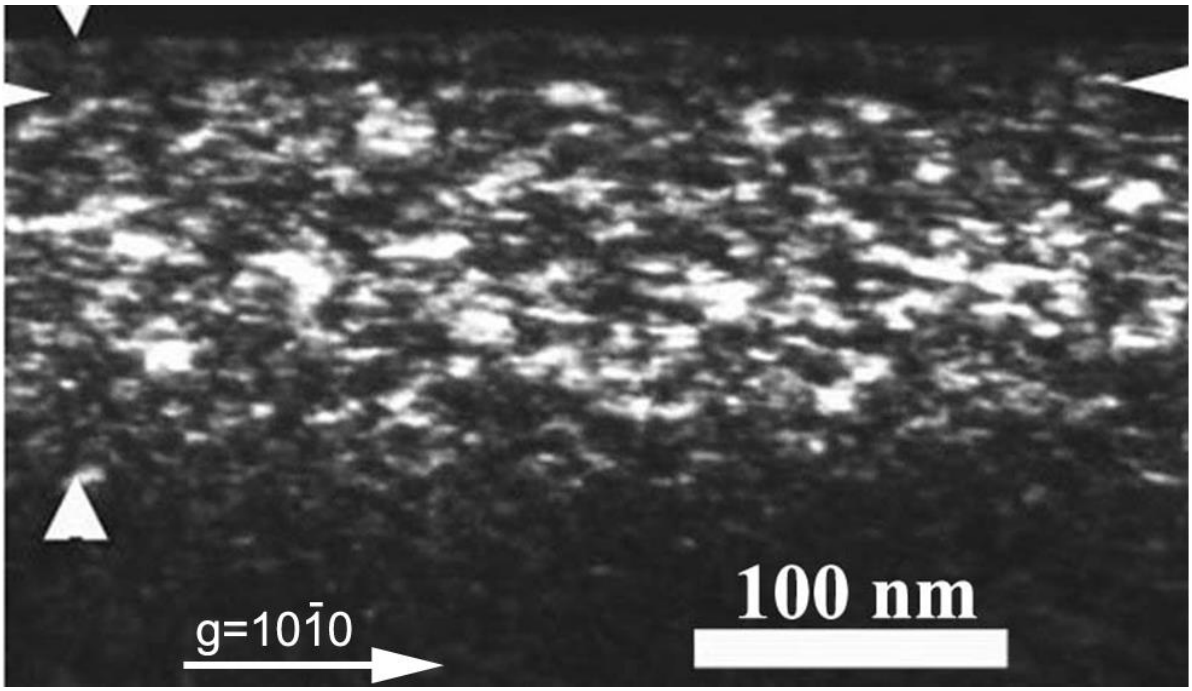

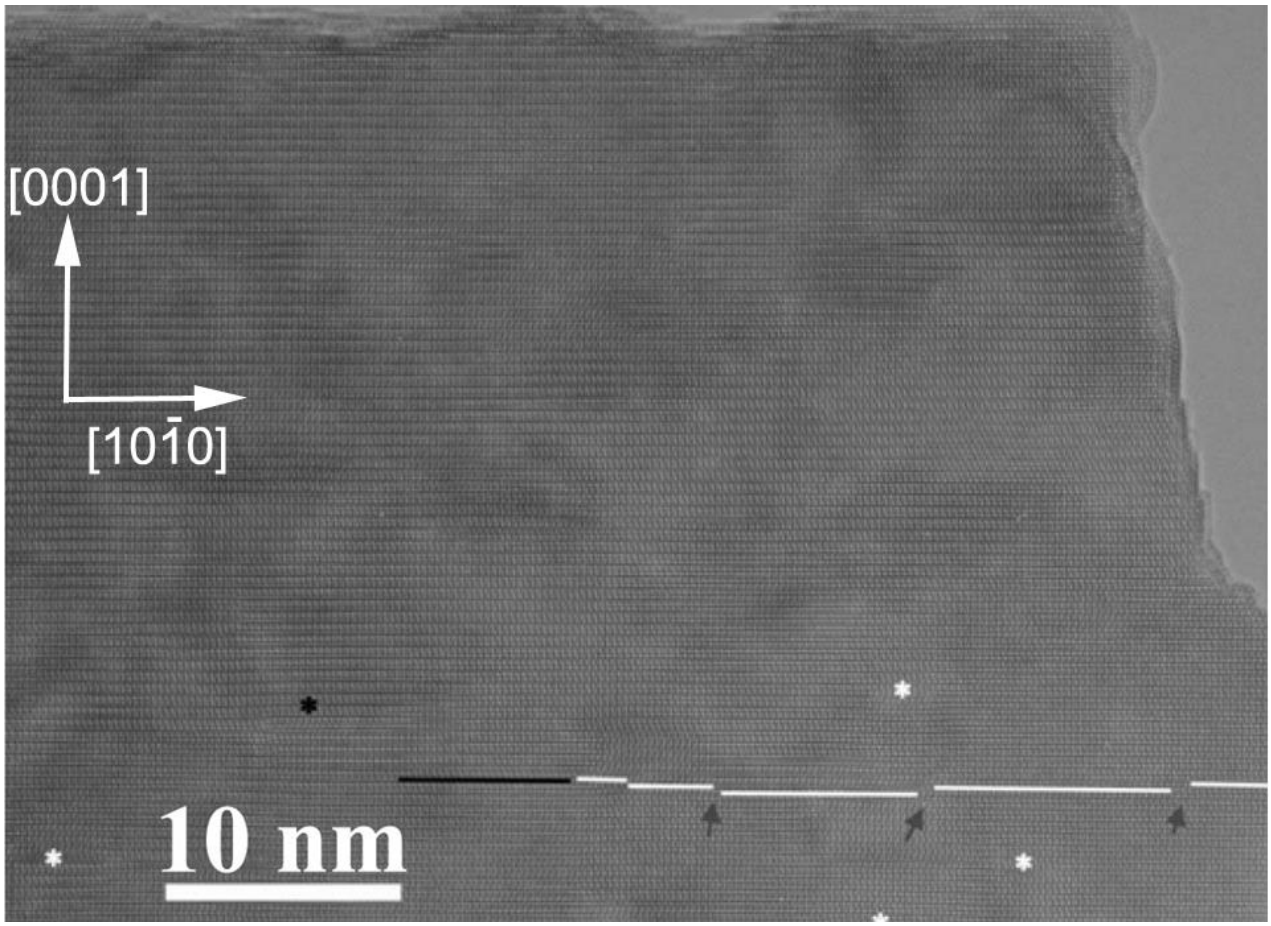
[0001]
[10$\bar{1}$0]
10 nm

Figure 4a

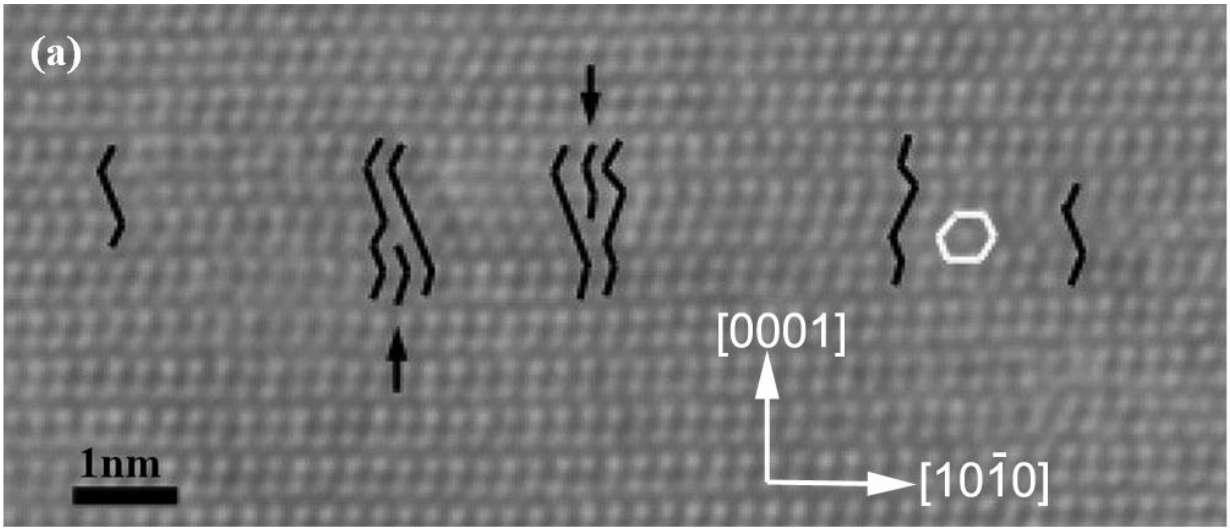

Figure 4b

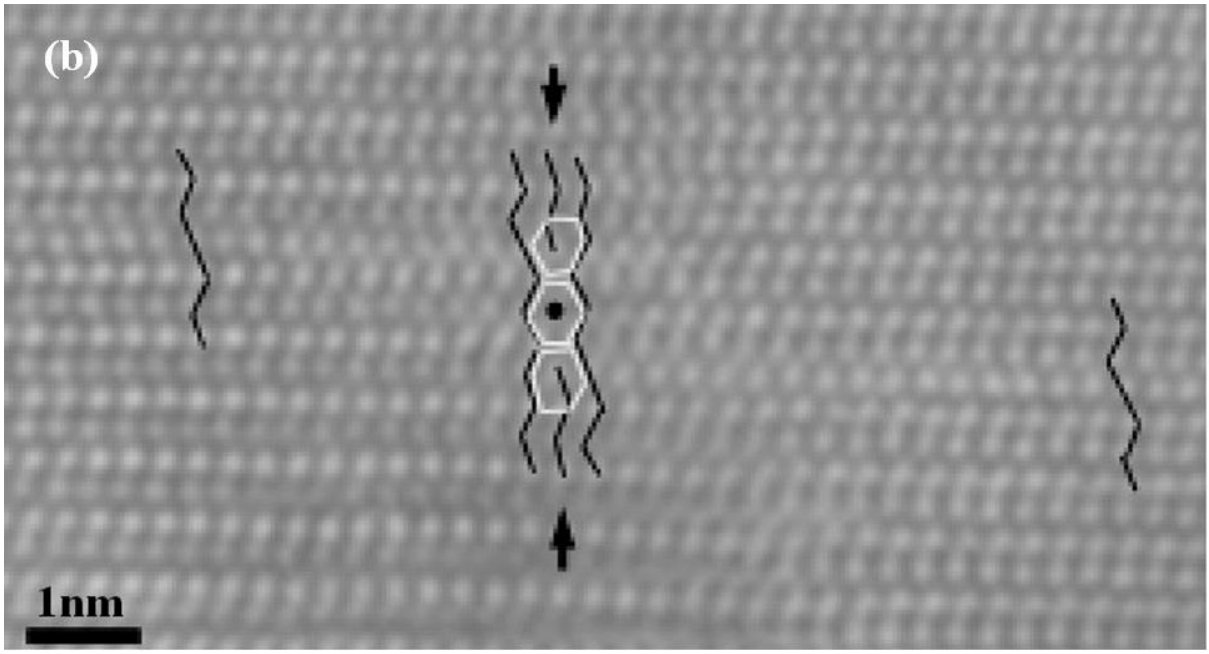

Figure 5

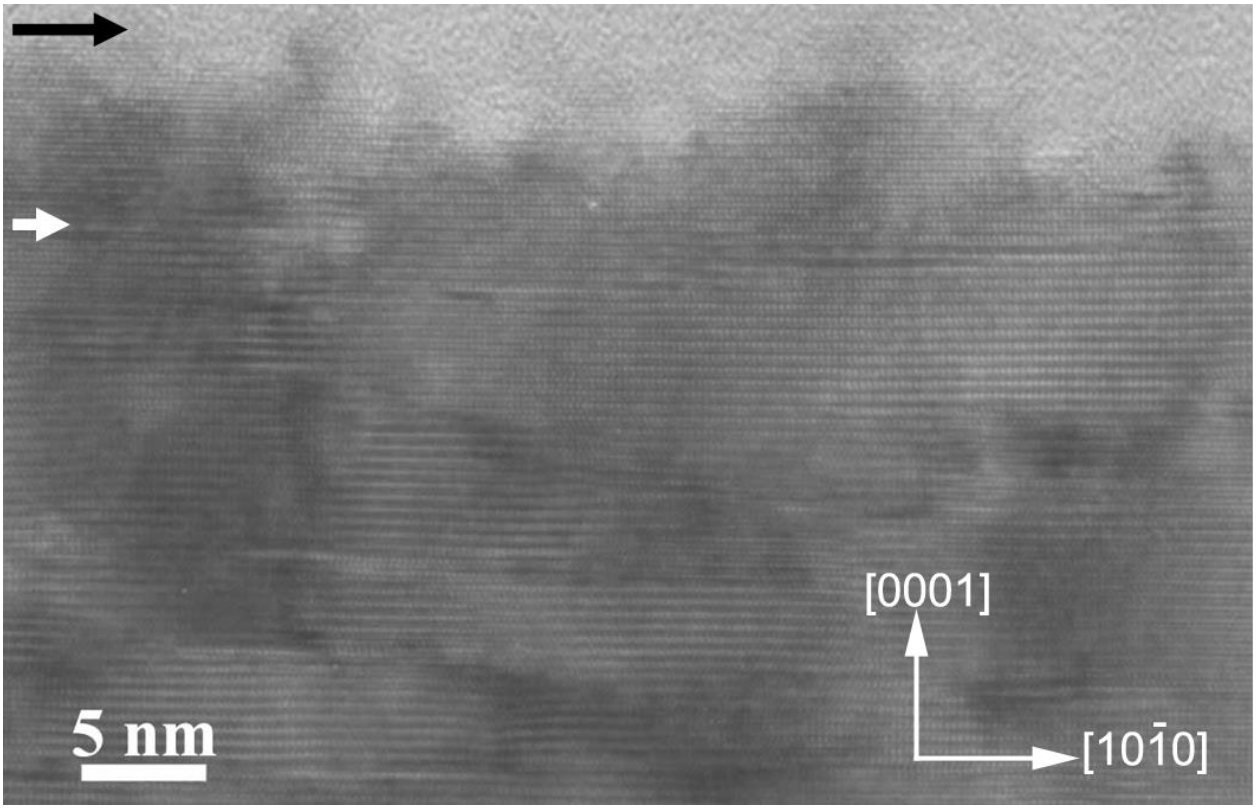

Figure 6

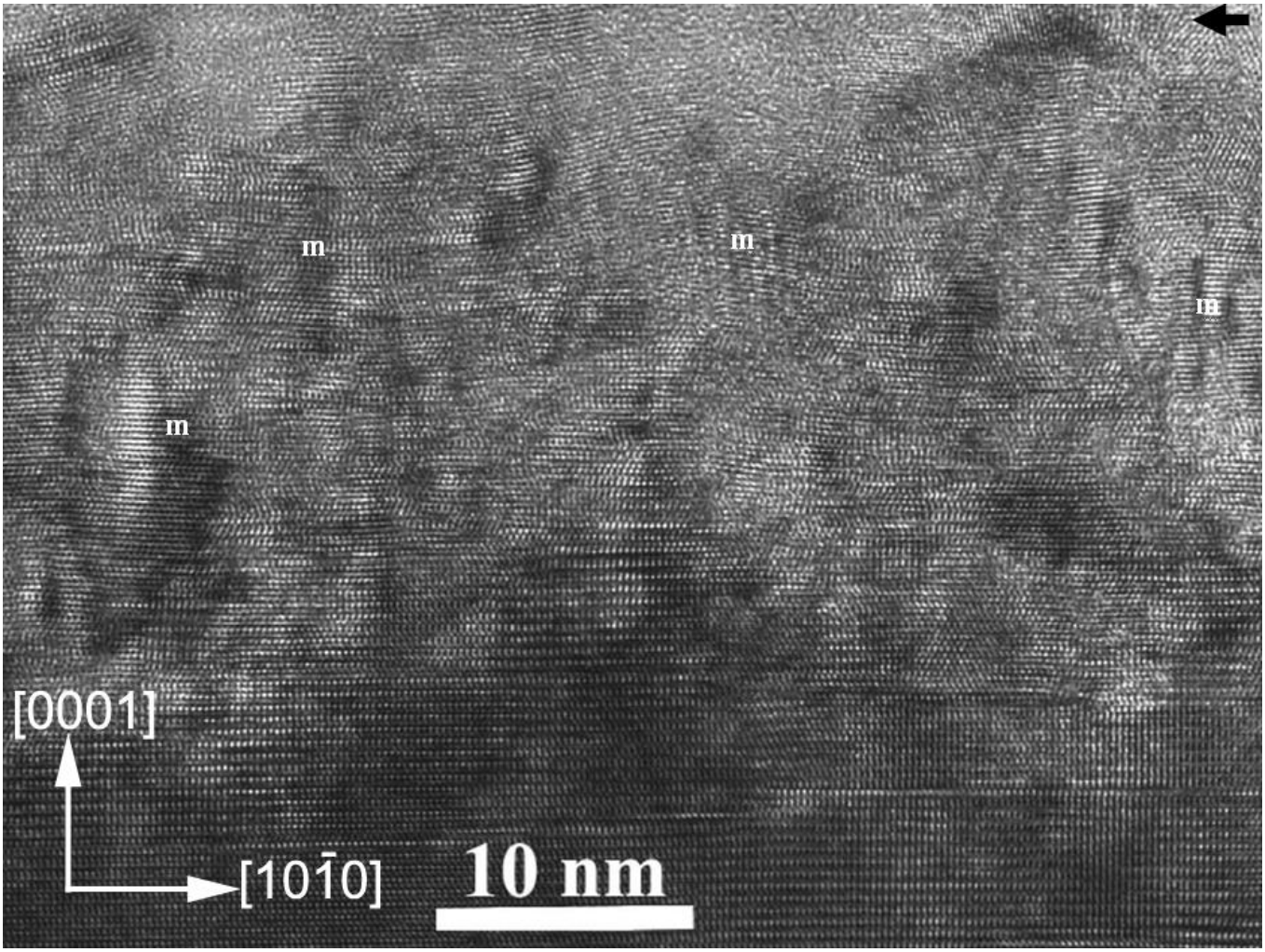

Figure 7a

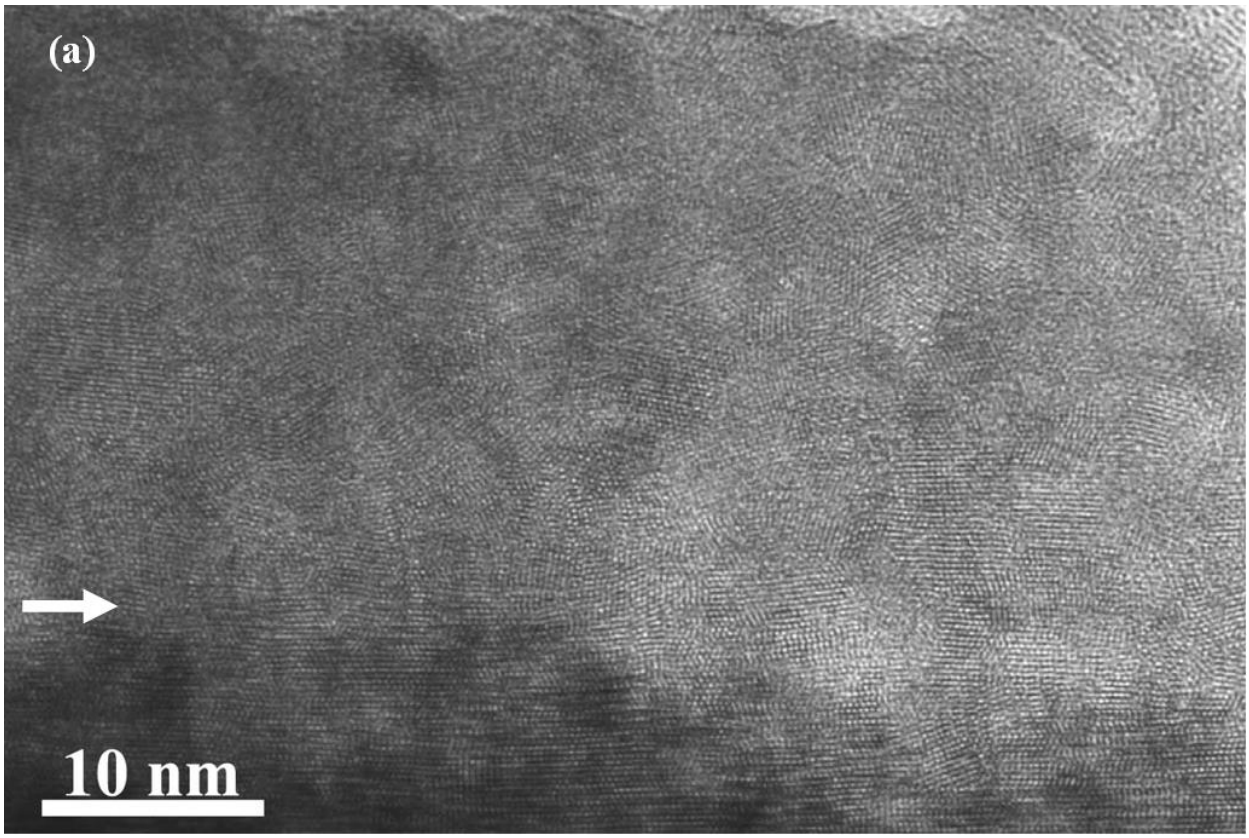

Figure 7b

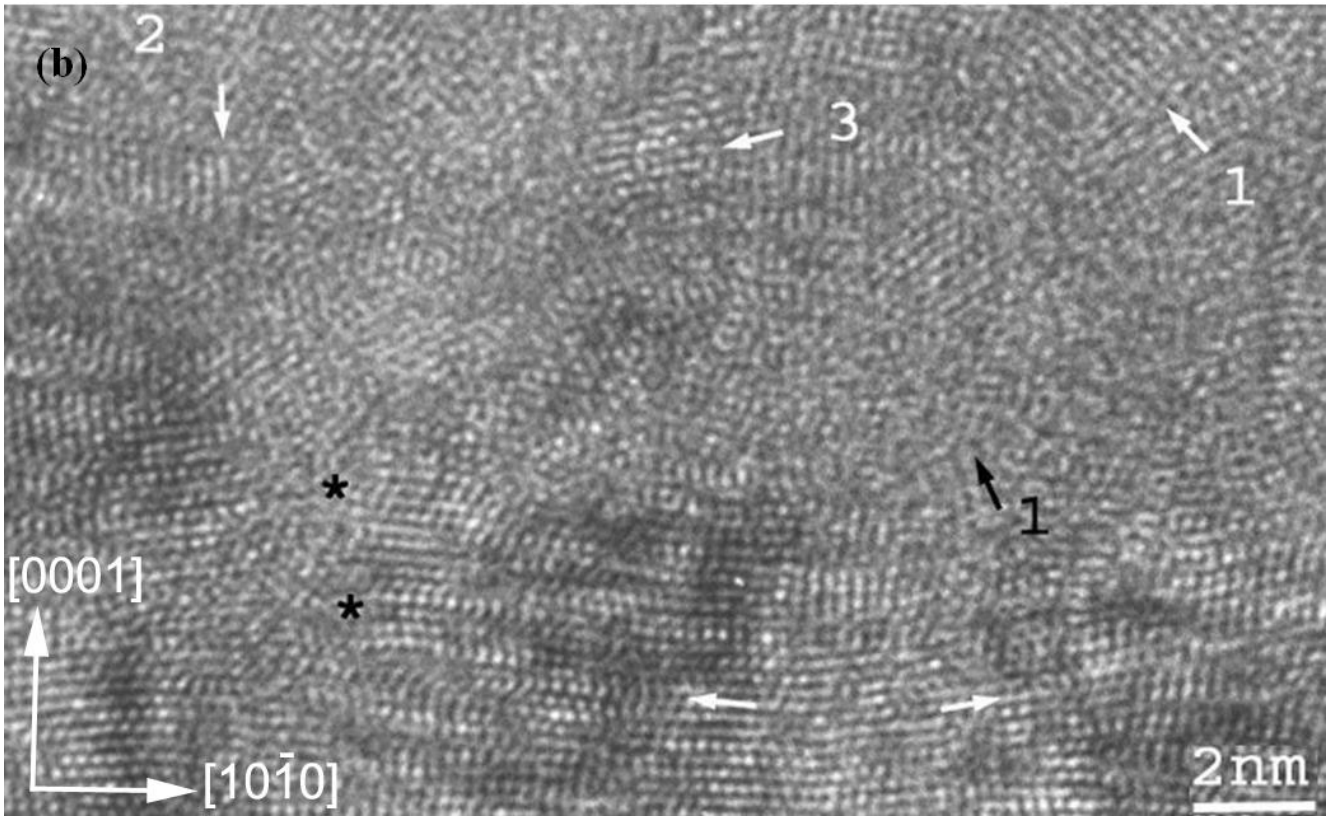

Figure 8

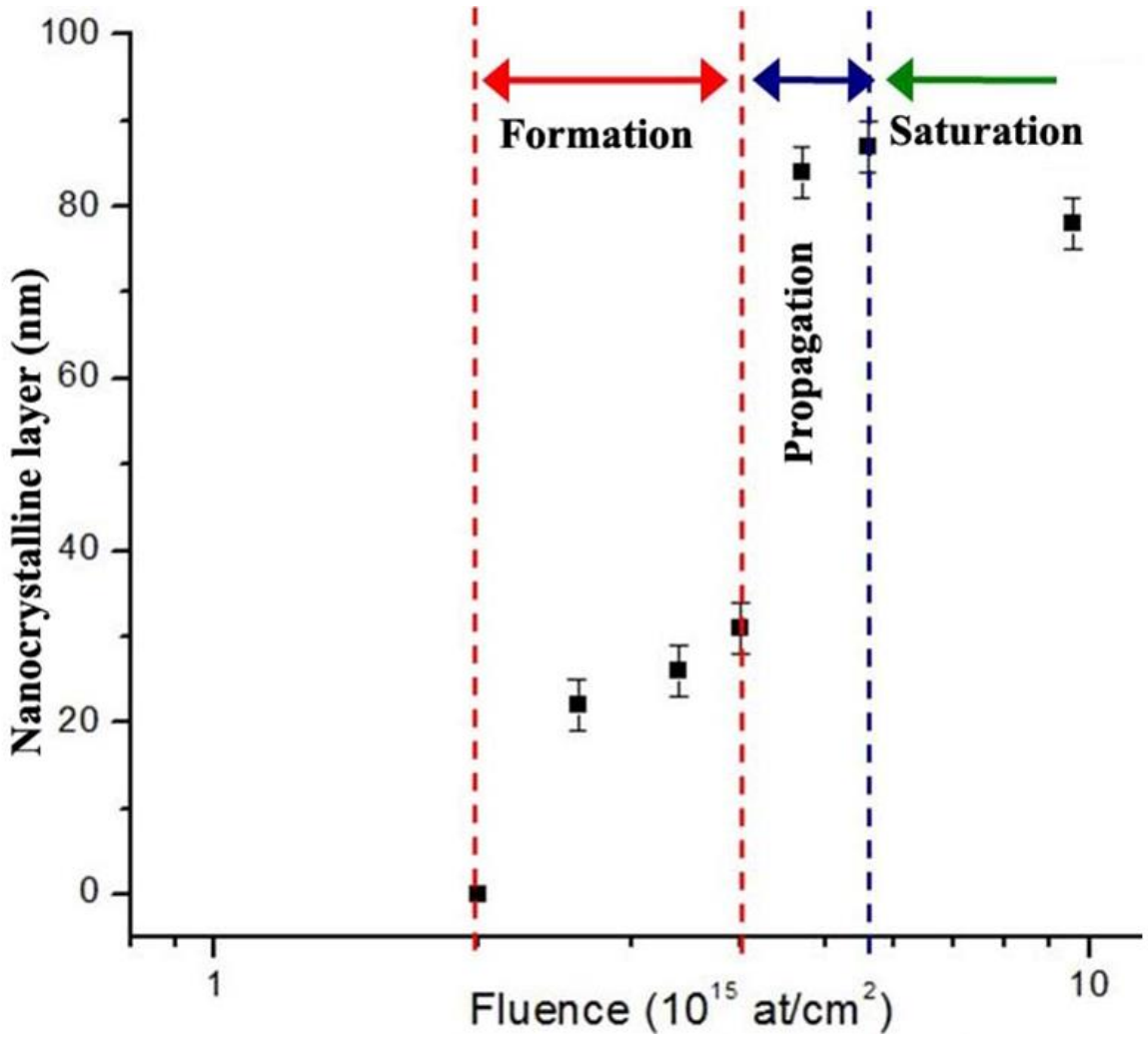
Formation
Propagation
Saturation
Nanocrystalline layer (nm)
100
80
60
40
20
0
1
10
Fluence (10^{15} at/cm^2)

Figure 9

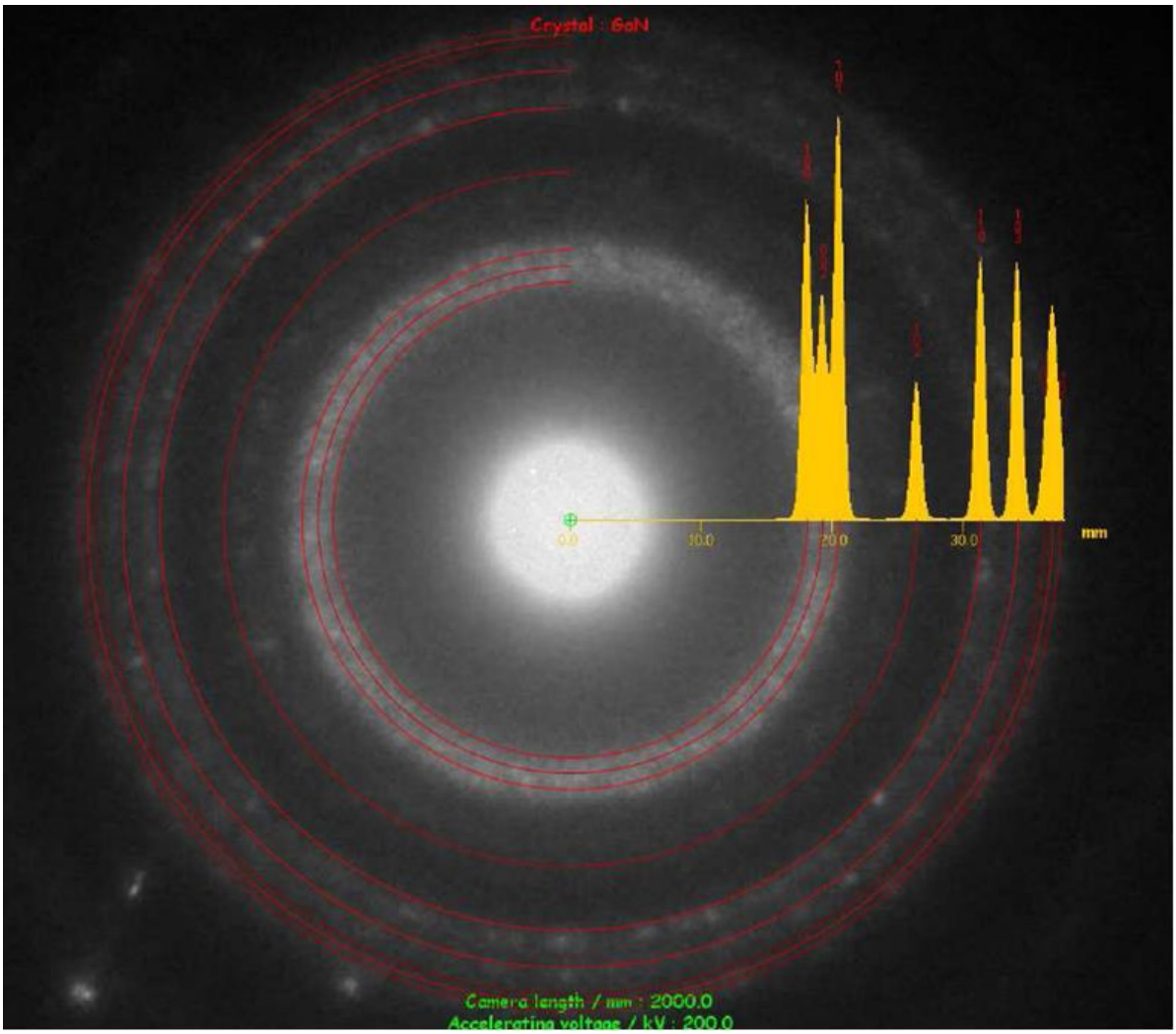
Crystal : GaN
0.0
10.0
20.0
30.0
mm
Camera length / mm : 2000.0
Accelerating voltage / kV : 200.0

Figure 10

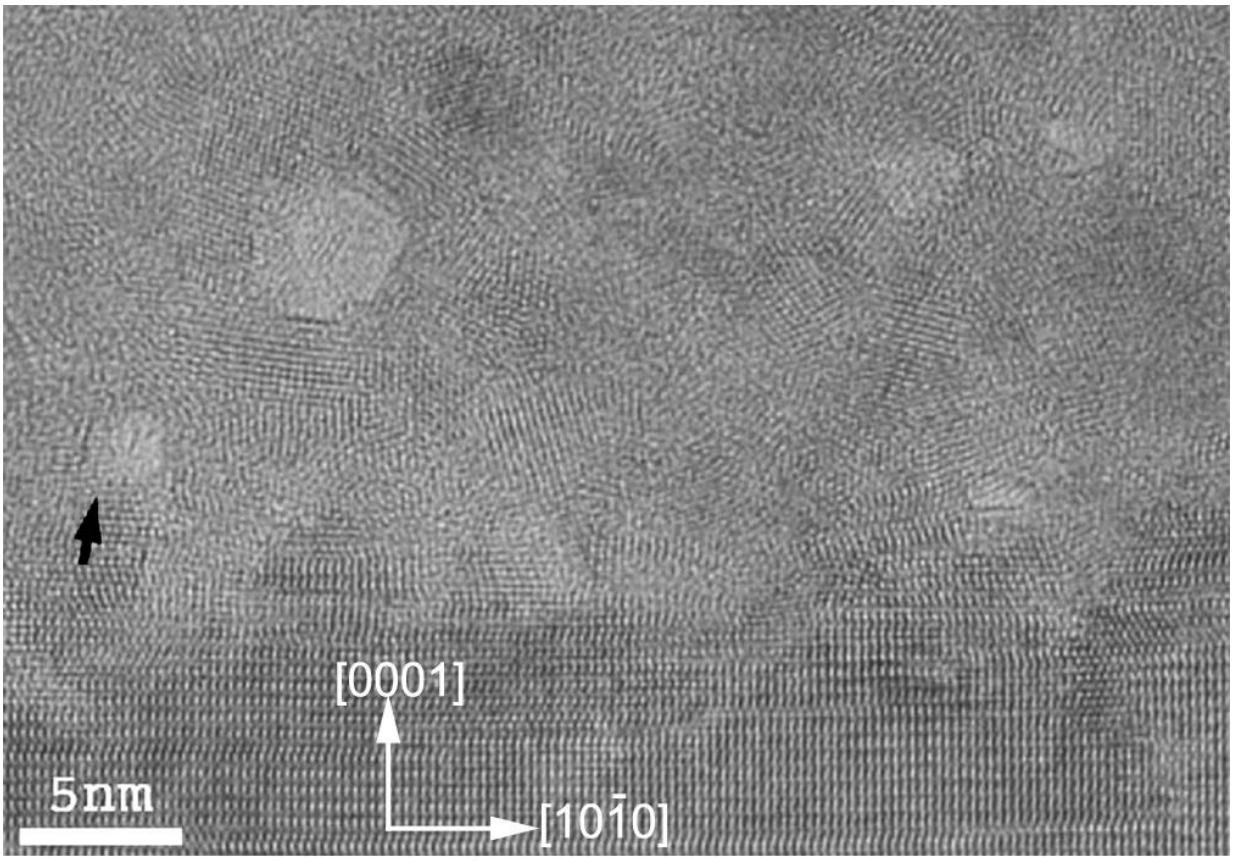

Figure 11

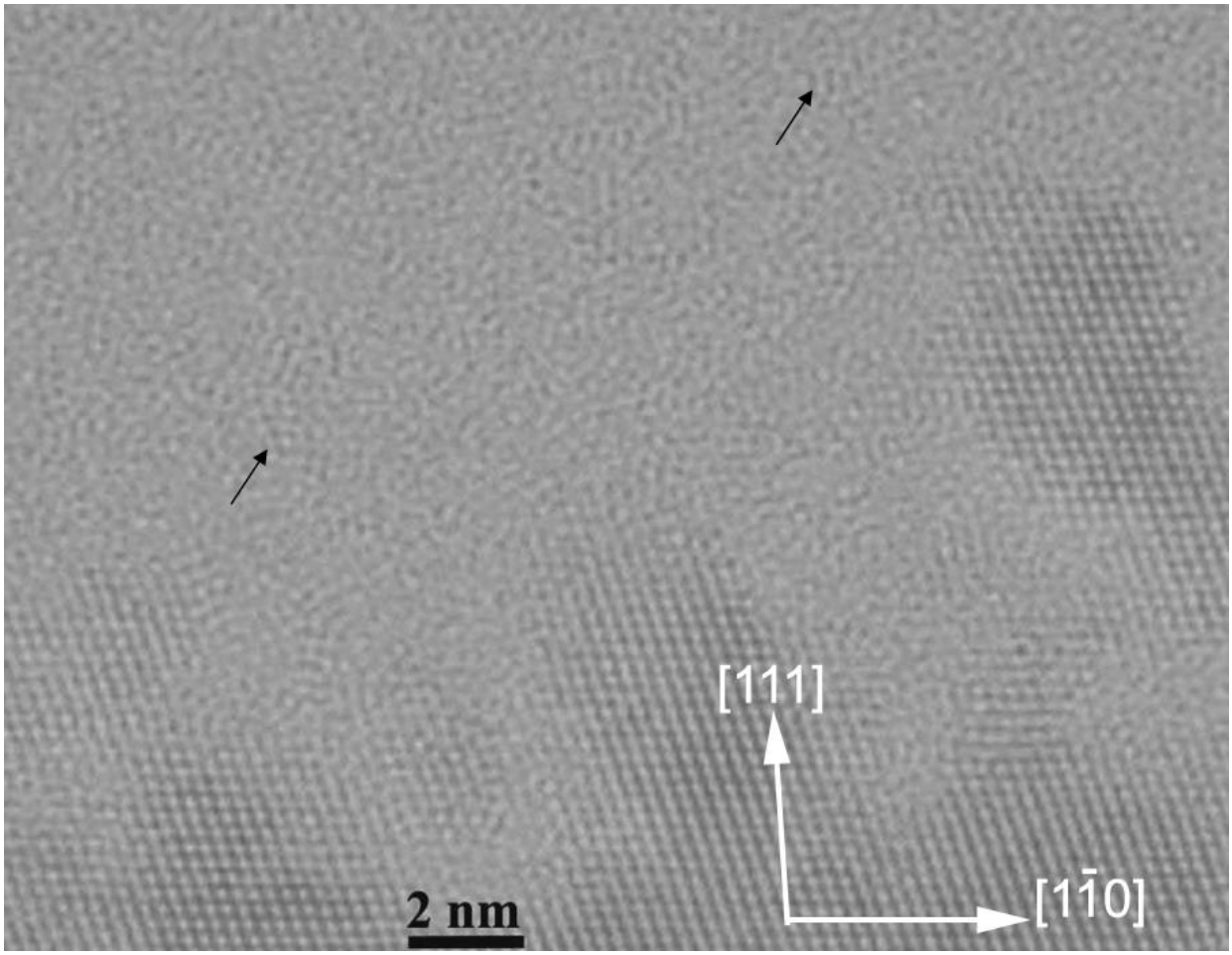

Figure 12a

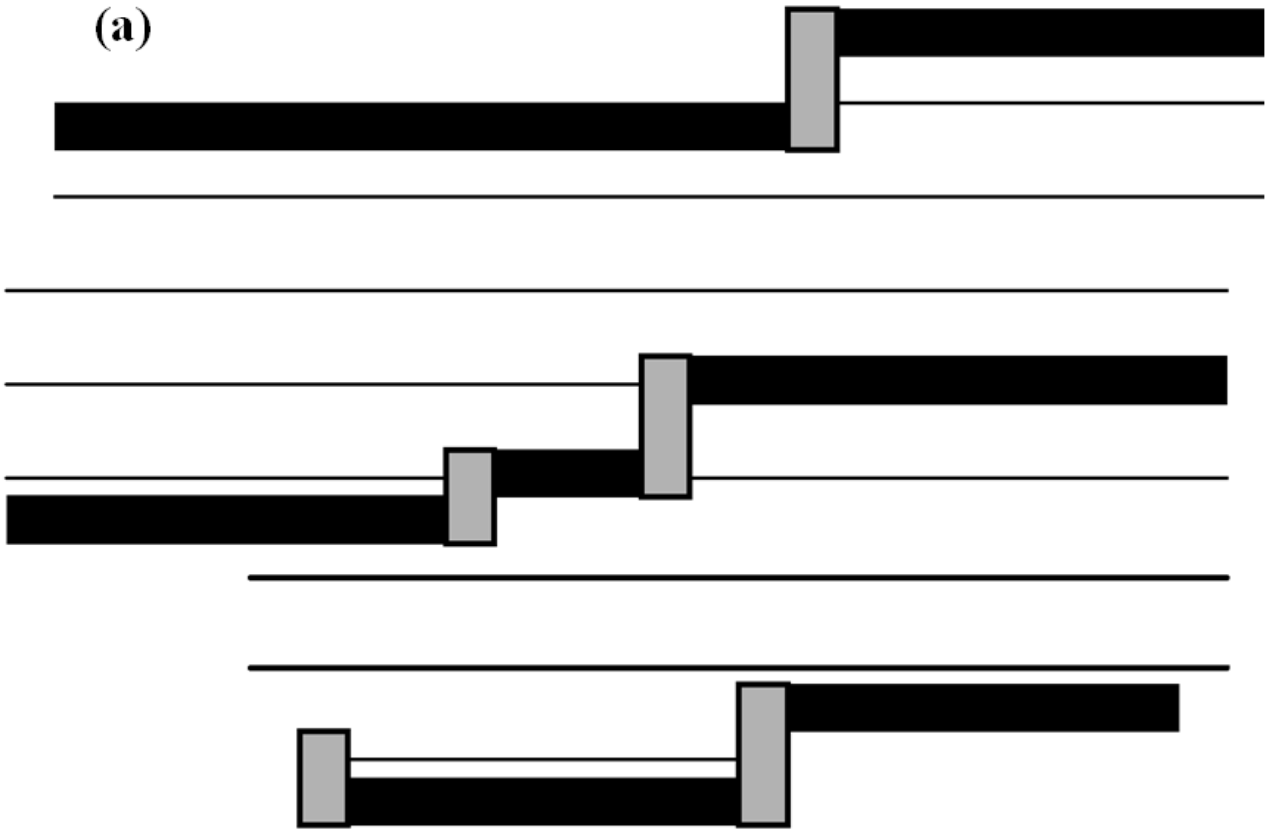

Figure 12b